Vol. **123** (2013) *ACTA PHYSICA POLONICA A* No. 5

Proceedings of the IX International Conference ION 2012, Kazimierz Dolny, Poland, June 25–28, 2012

Chemical Composition of Native Oxide Layers on In^+ Implanted and Thermally Annealed GaAs

M. Kulik[a,*], D. Kołodyńska[b], J. Żuk[a], F.F. Komarov[c] and J. Filiks[a]
[a]Institute of Physics, Maria Curie-Skłodowska University, pl. M. Curie-Skłodowskiej 1, 20-031 Lublin, Poland
[b]Department of Inorganic Chemistry, Faculty of Chemistry, Maria Curie-Skłodowska University
pl. M. Curie-Skłodowskiej 2, 20-031 Lublin, Poland
[c]Institute of Applied Physics Problems, Belarussian State University, Minsk, Belarus

Semi-insulating GaAs wafers have been implanted with 250 keV In^+ ions at a fluence of 3×10^{16} cm^{-2}. The samples prepared in this way were subsequently annealed at a temperature of 600 °C or 800 °C for 2 h. Thicknesses of the native oxide layers on implanted GaAs after samples storage in air were evaluated using the Rutherford backscattering spectrometry with the nuclear reaction $O^{16}(\alpha,\alpha)O^{16}$ method. The chemical composition of native oxide layers on In^+ implanted and annealed GaAs has been studied using X-ray photoelectron spectroscopy. As_2O_3, As_2O_5, Ga_2O_3, GaAs, InAs and $InAsO_4$ compounds were detected in these layers.

DOI: 10.12693/APhysPolA.123.943
PACS: 61.72.uj, 79.60.–i, 82.80.Yc

1. Introduction

In recent years much interest has been devoted to investigations of the chemical composition, thermal desorption processes, thermal annealing and chemical etching of oxide surface layers covering A_3B_5 crystals [1–3]. Transparent conducting oxides on semiconductor surfaces play an important role in electronics and optoelectronics, for example the indium oxide/n-GaAs junctions have been used in fabrication of diodes [2].

High quality layers of ternary $In_xGa_{1-x}As$ solid solutions are commonly grown on substrates of various A_3B_5 compounds, such as GaAs, InAs, InP using epitaxial techniques. Composition and concentration of the components in the ternary compounds can be controlled by ion implantation and post-implantation annealing conditions. The annealing is needed to recover a disordered crystalline structure and allow the implanted atoms to occupy specific sites in the lattice of A_3B_5 compounds [3].

In the paper the results of the study of subsurface layers of semi-insulating GaAs implanted with indium ions and subsequently annealed are presented.

2. Experimental

The samples of semi-insulating (SI) GaAs (100) were used in the experiment. SI GaAs wafers were chemicaly cleaned before ion implantation [4]. They were irradiated with 250 keV In^+ ions using the UNIMAS ion implanter at Maria Curie-Skłodowska University [5]. The fluence of implanted In^+ ions was 3×10^{16} cm^{-2} at the ion current density below 1 μA cm^{-2} to avoid *in situ* annealing. After ion implantation the sample surface was covered with a 100 nm thick protective layer of Si_3N_4. Thermal annealing process was carried out at temperatures: 600 °C or 800 °C. Annealing time was 2 h for both temperatures, and after the process the Si_3N_4 layers were chemically removed.

The post-implantation investigations have been performed by two nuclear methods: the Rutherford backscattering spectrometry (RBS) [6] and the nuclear reaction (NR) $O^{16}(\alpha,\alpha)O^{16}$ [7], and also X-ray photoelectron spectroscopy (XPS) [8]. The thickness of surface layers enriched in oxygen was determined using the NR method. The so called native oxide layers have been grown on surfaces of In^+ implanted GaAs in contact with ambient air during over one week storage. It was assumed that the native oxide layers are homogeneous and atomic concentrations are constant. The obtained values of layer thickness were less than 8.0 nm with the 0.5 nm accuracy. The RBS/NR spectra of the scattered α particles were collected for the following energies of the incident beam: 3.035, 3.045, 3.050, and 3.060 MeV. The detector resolution was 12 keV and the scattering angle $\theta = 170°$.

The chemical composition of the native oxide layers was analyzed by the XPS spectrometer equipped with the monochromatized Al K_α radiation [9]. The XPS spectra for all samples have been collected in the energy ranges: 38.5 to 48.5 eV, 101.0 to 113.0 eV, and 441.0 to 454.5 eV, according to the binding energies of As $3d$, Ga $3p$ and In $3d$, respectively. The measured bands were fitted with a Gaussian/Lorentzian function [10].

3. Results and discussion

The typical RBS/NR spectrum measured on the GaAs sample after In^+ implantation is shown in Fig. 1. Two features near the channel numbers: 330 and 850 are observed, assigned to α particles scattered on oxygen and

---

*corresponding author; e-mail: mkulik@hektor.umcs.lublin.pl

indium nuclei, respectively. It is also noticed that the edge in the vicinity of channel 800 consists of two steps (Figs. 1, 2). They are related to the α particles scattered on Ga and As nuclei. It was observed for all the measured samples that these edges near channel 800 are quite sharp. This fact can be explained by a good quality of the studied GaAs surfaces. The position of the band with respect to the implanted indium indicates that the atoms are in the near-surface layer. The results presented in [11] confirm that during the thermal annealing indium atoms diffuse to the surface and the atomic concentration of indium increases. At the same time, the decreasing scattering yield is observed in the part of the spectrum near channel number 800 for implanted and annealed GaAs (Fig. 2). This effect can be explained by the fact that arsenic atoms leave the surface layers during thermal annealing. The same effect was described in [12], where the XPS data measured for GaAs indicate the removal of As_2O_3 oxide after annealing at above 500 °C [13].

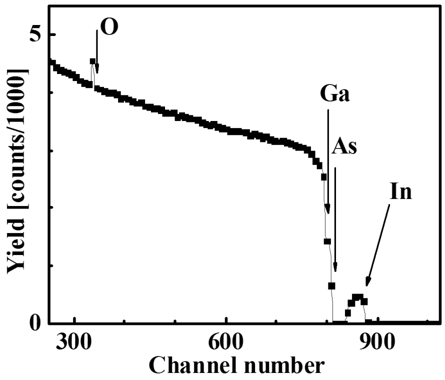

Fig. 1. RBS/NR spectrum of In^+ ion implanted GaAs.

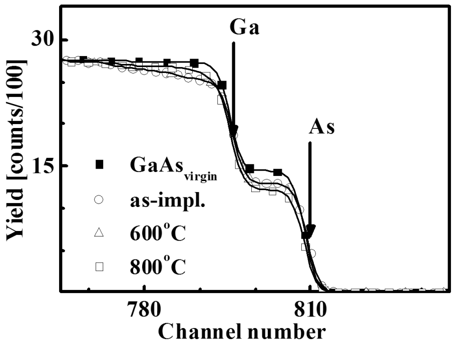

Fig. 2. Part of RBS spectra measured on virgin, In^+ implanted and annealed GaAs.

The thicknesses of the native oxide layers were determined using the RBS/NR method. Four spectra for energies of the α particles between 3.035 and 3.060 MeV have been collected, for each studied sample. Interesting parts of the spectra are presented in Fig. 3. It was found for all samples that the intensity of the oxygen band changes with the energy of α particles below and above the resonance energy $E_\alpha = 3.045$ MeV. This effect confirms that on the investigated surfaces there are thin layers containing oxygen atoms. They are homogeneous within the limits of a measurement error. It is observed that the collected spectra at $E_\alpha = 3.045$ MeV for all samples differ only in the yield of the band maximum at channel number 330. It indicates that the thicknesses of the native oxide layers on the investigated samples are different.

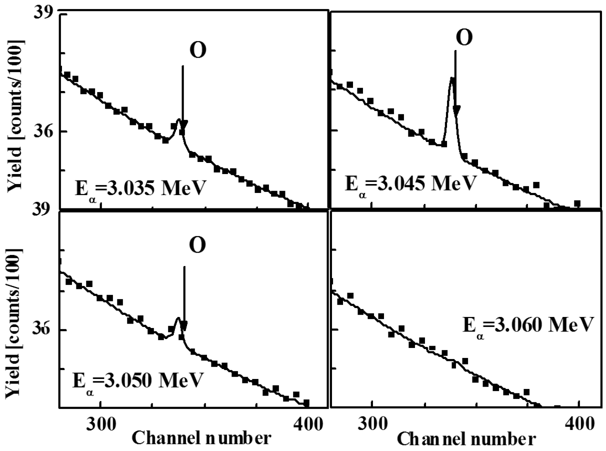

Fig. 3. Fragments of RBS/NR spectra collected for virgin GaAs near the band associated with the α particles scattered at oxygen atoms.

TABLE I

Thickness of native oxide layers on investigated samples.

GaAs samples		Thickness [nm] ±0.5 nm
virgin		4.2
implanted		7.6
annealed [°C]	600	7.1
	800	5.6

In the calculations it is assumed that the homogeneous native oxide layers have a sharp border between the layer and GaAs. The oxide layer thickness increases after implantation, and then it decreases following the thermal annealing at 800 °C (Table I). This behavior can be explained by oxidation of two kinds of implanted GaAs subsurface layers. The first one is structurally amorphous after In^+ ion implantation and the second kind of the layer after annealing, especially at 800 °C is characterized by at least moderate crystalline quality. The samples structure was rebuilt and enriched in indium [14].

It is known that due to the exposure of virgin GaAs samples to air at room temperature, oxidation of As atoms proceeds according to the reaction [15]:

$$4As + 3O_2 \rightarrow 2As_2O_3. \qquad (1)$$

The same is true for Ga atoms and a mixed oxide layer consisting of As_2O_3 (and then As_2O_5) and Ga_2O_3 is formed. As_2O_3 and As_2O_5 are the most unstable and they are easily removed and converted to Ga_2O_3. Their stability causes difficulty in their removal during typical chemical processing or thermal desorption at low temperatures.

Additionally, after implantation $InAsO_4$ and In_2O_3 are also formed. In order to predict composition of the mixture, the analysis of the Gibbs free energy is useful. The Gibbs free energy, being a function of the enthalpy and entropy changes, indicates which compounds under normal conditions are thermodynamically stable (having more negative values) [16]. Additionally, the thermodynamic analysis is also useful for determination of the type of reaction and whether or not the reaction will occur. Specifically, a value of the Gibbs free energy indicates whether the reaction is oxidizing, reducing or if the system is in equilibrium. Additionally, thermodynamic modeling can be used to study the effect of temperature, oxygen partial pressure, moisture etc. and their importance in oxide film growth. The analysis of these values also suggests the possibility of conversion of less stable oxides to more stable ones.

For example, at higher temperatures less stable arsenic oxides (As_2O_3, $\Delta G = -137.7$ kcal/mol and As_2O_5, $\Delta G = -187$ kcal/mol [11]) become less predominant in the system due to the evaporation process or conversion to the most stable oxides, e.g. Ga_2O_3, $\Delta G = -238.6$ kcal/mol [16].

As_2O_5 is present only on significantly oxidized samples due to its high oxidation state and decomposes at temperature in the range 250–300 °C. Therefore, the conversion process can be summarized according to the reactions

$$3As_2O_5 + 4GaAs \rightarrow 3As_2O_3 + 2Ga_2O_3 + 4As, \quad (2)$$

$$2As_2O_5 + GaAs \rightarrow GaAsO_4 + As_2O_3. \quad (3)$$

For $GaAsO_4$ the Gibbs free energy is equal to -212.8 kcal/mol [16]. As follows from the literature data and the phase diagram [11, 16], in the system probable existence of Ga_2O ($\Delta G = -75.3$ kcal/mol), $GaAsO_4$ ($\Delta G = -212.8$ kcal/mol) and less possibly $Ga(AsO_3)_3$ and GaO as well as bonding configurations similar to unstable species such as As_2O, AsO and As_2O_4 should be also taken into account. The temperature of $GaAsO_4$ decomposition is unknown. Probably, it should be at lower temperatures, according to the following reaction:

$$2GaAsO_4 \rightarrow Ga_2O_3 + As_2O_3 + O_2 \uparrow . \quad (4)$$

Decomposition of As_2O_3 occurs when the oxide is heated to temperatures between 285–500 °C:

$$As_2O_3 + 2GaAs \rightarrow Ga_2O_3 + 4As. \quad (5)$$

Therefore after the post-implantation annealing at 600 °C the intensity of Ga_2O_3 peaks in the XPS spectra should increase significantly.

Moreover, Ga_2O_3 when heated to a temperature in the range of 550–700 °C is expected to decompose according to

$$Ga_2O_3 + 4GaAs \rightarrow 3Ga_2O \uparrow + 4As \uparrow . \quad (6)$$

The elemental As is localized at the oxide–GaAs interface, although some of As atoms may subsequently diffuse through Ga_2O_3 to form $GaAsO_4$ regions. It was found that arsenic atoms concentration also decreases during thermal annealing, the same results were described in [17]. Any arsenic oxides that may be formed via this elemental arsenic diffusion to the surface are likely to be highly unstable and therefore easily evaporate.

It should be also mentioned that the chemisorption of atomic oxygen onto gallium arsenide is based on the atomic oxygen insertion between gallium–arsenic bonds (As–O–Ga), adjacent gallium–arsenic bonds, gallium–gallium bonds on defect sites (Ga–O–Ga) and non-bridging atomic oxygen (As=O or Ga=O) [18–20].

Under analogous condition formation of stable metal oxides $InAsO_4$ ($\Delta G = -209.4$ kcal/mol) and In_2O_3 ($\Delta G = -198.6$ kcal/mol) was reported. However, for thermally grown oxides at above 350 °C, the oxide consists almost entirely of ternary $InAsO_4$ [12].

The XPS spectra of virgin GaAs as well as for the samples after ion implantation and thermal treatment at 600 °C and 800 °C are presented in Fig. 4. Two As 3*d* lines, one near the energy 41.5 eV and the second at about 45.5 eV are observed (Fig. 4a). They are connected with As bonds in GaAs, As_2O_3 and As_2O_5. The intensity of these bands suggests that the concentration of arsenic oxides is higher compared to that of GaAs.

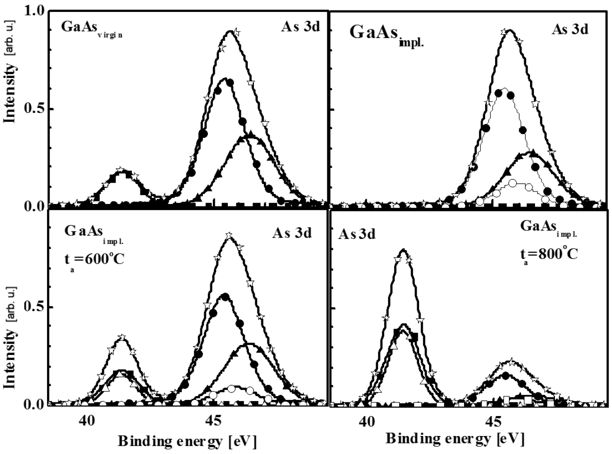

Fig. 4. Experimental and best-fitted XPS spectra for all samples (As 3*d* band). Solid line — best fit, stars — measurement. The deconvolution results: (■) GaAs, (●) As_2O_3, (▲) As_2O_5, (△) InAs, (□) $InAsO_4$.

The obtained results were confirmed by the XPS spectrum measured near the Ga 3*p* band (Fig. 5). The spectrum has been fitted with 3 bands attributed to Ga bonds in Ga_2O_3 and GaAs compounds. From the XPS results described above we can conclude that the native oxide layer on the virgin GaAs surface is a mixture of Ga_2O_3, As_2O_3, As_2O_5 and GaAs compounds.

Additionally, it is found that after the implantation and thermal annealing the relative intensities of the lines

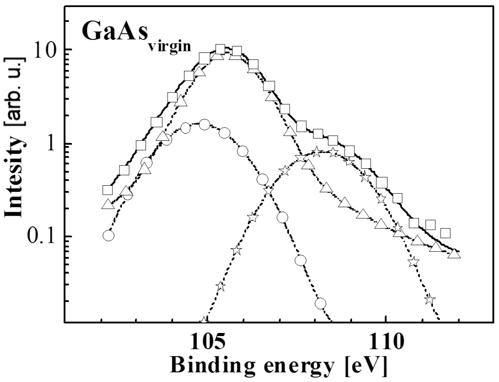

Fig. 5. Experimental and best-fitted XPS spectrum (Ga $3p$ band) from native oxide on unimplanted GaAs: (□) measured values, solid line — best fit. The dashed lines — after deconvolution, Ga $3p_{3/2}$: circles — GaAs, triangles — Ga_2O_3 and Ga $3p_{1/2}$ stars — GaAs.

are changed (Fig. 4b–d). Table II presents the calculated values of peak areas corresponding to the Ga $3p$ bands in GaAs and Ga_2O_3. The influence of ion implantation and annealing on composition of the oxide layers is very strong.

TABLE II

Ga $3p$ band areas obtained from the best fit to the XPS spectra measured from 101.0 to 113.0 eV.

Sample	Peak area [arb. u.]		
	Ga $3p_{3/2}$		Ga $3p_{1/2}$
	GaAs	Ga_2O_3	GaAs
virgin GaAs	4.330	20.556	2.224
implanted GaAs	0.059	23.594	0.027
impl. anneal. GaAs			
600 °C	0.963	22.299	0.438
800 °C	1.311	20.969	0.656

TABLE III

In $3d$ band areas obtained from the best fit to the XPS spectra in the 441 to 454 eV energy range.

Sample	Peak area [arb. u.]			
	In_2O_3 $3d_{5/2}$	InAs $3d_{5/2}$	InAs $3d_{5/2}$	$InAsO_4$ $3d$
virgin GaAs	0.0	0.0	0.0	0.0
implanted GaAs	3.420	0.0	0.0	4.760
impl. anneal. GaAs				
600 °C	2.930	10.282	5.853	3.621
800 °C	2.157	12.450	7.135	1.692

Comparing the intensity of the lines in Fig. 4c and d we find that they change with the increasing temperature of annealing. This is accompanied by arsenic oxides disappearance and InAs and GaAs compounds increase. During thermal annealing InAs and GaAs are formed in the surface layers. These effects are in a good agreement with the results showing the increase of arsenic concentration in the near surface layers as presented in Fig. 2 (RBS measurements). However, the intensity of lines in Fig. 4c and d is different which indicates that the content of As oxides decreases in the native oxide layer. Additionally, it is observed that the lines As $3d$ and Ga $3p$ assigned to GaAs disappear after implantation and the band of In $3d$ appears (Fig. 6). The band is superposition of In $3d$ lines in indium oxides: In_2O_3 and $InAsO_4$. This effect can be due to amorphous subsurface layer and connected with the diffusion of indium atoms to the surface during implantation.

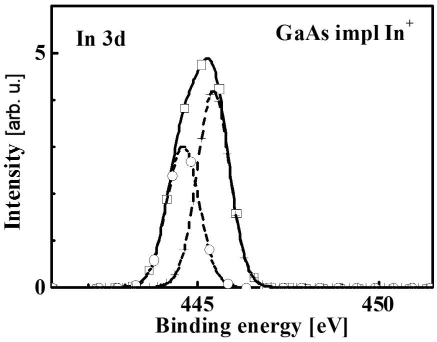

Fig. 6. Experimental and best-fitted XPS In $3d$ band from native oxide on implanted GaAs: (□) measured values, solid line — best fit. Deconvolution results: (○) In_2O_3, (+) $InAsO_4$.

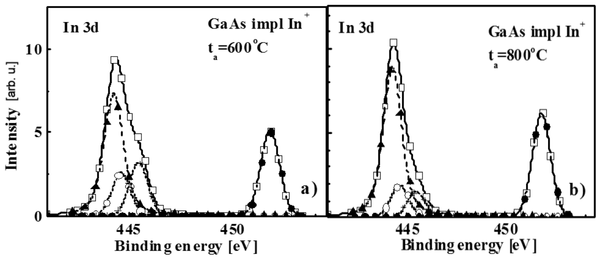

Fig. 7. Experimental and best-fitted XPS spectra of In $3d$ bands from native oxide on implanted and annealed at 600 (a) and 800 °C (b) GaAs samples: (□) experimental results, lines — the best fit. Deconvolution results: (○) In_2O_3 $3d_{5/2}$, (▲) InAs $3d_{5/2}$, (●) InAs $3d_{1/2}$, (+) $InAsO_4$ $3d$.

The process of thermal annealing leads to appearance of a line at 452 eV (Fig. 7). This corresponds to formation of InAs in the surface layer during post-implantation thermal annealing. The band shape at about 445 eV evolves also during rebuilding of the implanted layers. This effect can be explained by transformation of indium compounds from In_2O_3 and $InAsO_4$ to InAs with the increase of annealing temperature, which is correlated with the Gibbs free energy. The intensity of lines In $3d$ referred to InAs also increases with the temperature annealing growth (see Table III). This effect is confirmed by the increase of the peak area in Fig. 7.

4. Conclusion

Investigations of a few nanometer thick native oxide layers on In$^+$-implanted and annealed at 600 °C or 800 °C GaAs have shown formation of InAs compound in the native oxide layer. As_2O_3, As_2O_5, Ga_2O_3, and GaAs compounds were also detected by XPS in native oxides on virgin and ion-implanted GaAs. Following In$^+$-ion implantation, In_2O_3 and $InAsO_4$ become present in the native oxide layer. After annealing, the In 3*d* line from InAs starts to dominate the XPS spectra. Most probably indium atoms diffuse to the surface during thermal treatment and the atomic concentration increases in the near surface layer, however, the atomic concentration of arsenic decreases. This is the evidence that the arsenic atoms leave the disordered near-surface layer during implantation.

References

[1] D.A. Allwood, R.T. Carline, N.J. Mason, C. Pickering, B.K. Tanner, P.J. Walker, *Thin Solid Films* **364**, 33 (2000).

[2] A. Golan, J. Bregman, Y. Shapira, M. Eizenberg, *J. Appl. Phys.* **69**, 1494 (1991).

[3] A.N. Akimov, L.A. Vlasukova, F.F. Komarov, M. Kulik, *J. Appl. Spectrosc.* **59**, 533 (1993).

[4] D.E. Aspnes, A.A. Studna, *Phys. Rev. B* **27**, 985 (1983).

[5] M. Turek, S. Prucnal, A. Drozdziel, K. Pyszniak, *Rev. Sci. Instrum.* **80**, 043304 (2009).

[6] L.C. Feldman, J.W. Mayer, *Fundamentals of Surface and Thin Film Analysis*, North-Holland, New York 1986.

[7] J.R. Cameron, *Phys. Rev.* **90**, 839 (1953).

[8] W. Olovsson, T. Marten, E. Holmstrom, B. Johansson, I. Abrikosov, *J. Electron Spectrosc. Relat. Phenom.* **178**, 88 (2010).

[9] M. Kulik, S.O. Saied, J. Liskiewicz, *Nukleonika* **44**, 167 (1999).

[10] M. Procop, *J. Electron Spectrosc. Relat. Phenom.* **59**, R1 (1992).

[11] A.J. Bard, R. Parsons, J. Jordan, *Standard Potentials in Aqueous Solutions*, Marcel Dekker, New York 1985.

[12] S. Oktyabrsky, P. Ye, *Fundamentals of III–V Semiconductor MOSFETs*, Springer, 2010.

[13] F. Shi, K.L. Chang, K.C. Hsieh, *Proc. Institution of Mechanical Engineers, Part N: J. Nanoengin. Nanosys.* **221**, 37 (2007).

[14] M. Kulik, A.P. Kobzev, D. Jaworska, J. Zuk, J. Filiks, *Vacuum* **81**, 1124 (2007).

[15] P.A. Bertrand, *J. Vacuum Sci. Technol.* **18**, 28 (1981).

[16] G. Hollinger, R.S. Kabbani, M. Gendry, *Phys. Rev. B* **49**, 11159 (1994).

[17] H. Morota, S. Adachi, *J. Appl. Phys.* **105**, 123520 (2009).

[18] K. Nakajima, J. Okazaki, *J. Electrochem. Soc.* **132**, 1424 (1985).

[19] K.A. Bertness, W.G. Petro, J.A. Silberman, D.J. Friedman, W.E. Spicer, *J. Vacuum Sci. Technol.* **3**, 1464 (1985).

[20] A. Ismail, J.M. Palau, L. Lassabatere, *J. Appl. Phys.* **60**, 1730 (1986).